

Connecting Binuclear Pd(III) and Mononuclear Pd(IV) Chemistry by Pd–Pd Bond Cleavage

David C. Powers,[†] Eunsung Lee,[†] Alireza Ariafard,^{‡,§} Melanie S. Sanford,^{||} Brian F. Yates,^{*,‡} Allan J. Canty,^{*,‡} and Tobias Ritter^{*,†}

[†]Department of Chemistry and Chemical Biology, Harvard University, 12 Oxford Street, Cambridge, Massachusetts 02138, United States

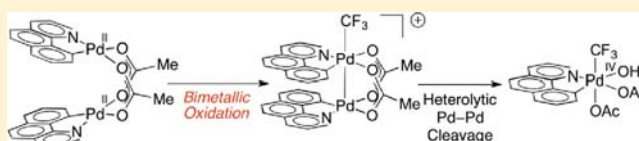
[‡]School of Chemistry, University of Tasmania, Private Bag 75, Hobart, Tasmania 7001, Australia

[§]Department of Chemistry, Faculty of Science, Central Tehran Branch, Islamic Azad University, Shahrak Gharb, Tehran, Iran

^{||}Department of Chemistry, University of Michigan, 930 North University Avenue, Ann Arbor, Michigan 48109, United States

S Supporting Information

ABSTRACT: Oxidation of binuclear Pd(II) complexes with PhICl_2 or $\text{PhI}(\text{OAc})_2$ has previously been shown to afford binuclear Pd(III) complexes featuring a Pd–Pd bond. In contrast, oxidation of binuclear Pd(II) complexes with electrophilic trifluoromethylating (“ CF_3^+ ”) reagents has been reported to afford mononuclear Pd(IV) complexes. Herein, we report experimental and computational studies of the oxidation of a binuclear Pd(II) complex with “ CF_3^+ ” reagents. These studies suggest that a mononuclear Pd(IV) complex is generated by an oxidation–fragmentation sequence proceeding via fragmentation of an initially formed, formally binuclear Pd(III), intermediate. The observation that binuclear Pd(III) and mononuclear Pd(IV) complexes are accessible in the same reactions offers an opportunity for understanding the role of nuclearity in both oxidation and subsequent C–X bond-forming reactions.

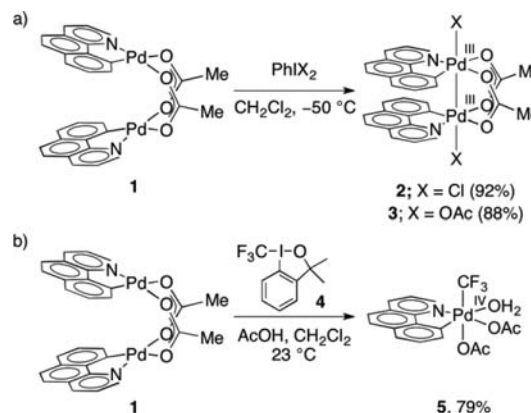


INTRODUCTION

Both mononuclear Pd(IV) and binuclear Pd(III) complexes can participate in C–X bond-forming reductive elimination reactions.^{1,2} Since 1971, mononuclear Pd(IV) complexes have been proposed as intermediates in a variety of Pd-catalyzed C–H functionalization reactions.^{3,4} Recently, both Ritter and Sanford have suggested that some reactions that were thought to proceed through mononuclear Pd(IV) intermediates may instead involve binuclear Pd(III) intermediates.^{2,5} Metal–metal (M–M) redox synergy during catalysis has been hypothesized to provide access to low-activation-energy redox processes in C–X bond-forming reactions.^{2e,5} Experimental and theoretical studies have suggested that C–X reductive elimination from binuclear Pd(III) complexes can be facilitated by M–M redox synergy.^{2e,6} Understanding the roles of mono- and binuclear intermediates in oxidation during catalysis could prove important for the design of new oxidative Pd-catalyzed C–X bond-forming reactions.

In 2009, Powers and Ritter reported that oxidation of binuclear Pd(II) complex **1** with I(III) oxidants PhICl_2 and $\text{PhI}(\text{OAc})_2$ affords binuclear Pd(III) complexes **2** and **3**, respectively (Scheme 1a).^{2a,c} In the same year, Sanford reported a kinetic analysis of a Pd(OAc)₂-catalyzed oxidation reaction with diaryliodonium salts, and also found evidence for binuclear Pd intermediates.^{2b} On the basis of these observations, binuclear Pd(III) intermediates were proposed in catalysis.^{2d,f,5} In 2010, Sanford reported that treatment of binuclear complex **1** with Togni’s I(III) reagent **4**⁷ affords

Scheme 1. (a) Oxidation of Binuclear Pd(II) Complex 1 with I(III)-Based Oxidants PhICl_2 or $\text{PhI}(\text{OAc})_2$ Results in the Formation of Binuclear Pd(III) Complex 2 or 3, Respectively, and (b) Oxidation of Binuclear Pd(II) Complex 1 with I(III)-Based Reagent 4 Affords Mononuclear Pd(IV) Complex 5



mononuclear Pd(IV) complex **5** (Scheme 1b).^{8,9} The formation of mononuclear Pd(IV) complex **5** under conditions similar to those previously identified to afford binuclear Pd(III) complexes raised questions regarding the generality of binuclear

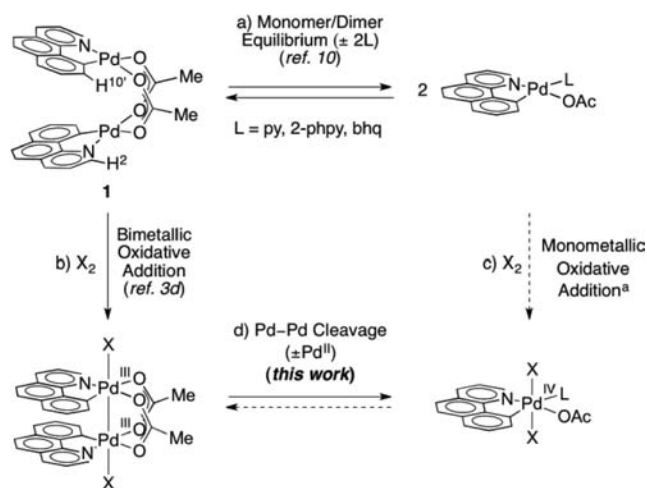
Received: July 21, 2011

Published: July 17, 2012

Pd intermediates in catalysis as well as the prospect that both binuclear Pd(III) and mononuclear Pd(IV) complexes may be accessible in the same oxidation reactions.

In an effort to understand the identity of high-valent intermediates in oxidative Pd catalysis, and in particular the potential interconversion of binuclear and mononuclear structures, we have pursued an investigation of the mechanism of the oxidation of **1** to afford **5**. Formation of mononuclear Pd(IV) complex **5** by oxidation of binuclear Pd(II) complex **1** could, in principle, proceed by either fragmentation of **1** to afford mononuclear Pd(II) complexes (reaction a, Scheme 2)

Scheme 2. Formation of Mononuclear Pd(IV) Complex 5 by Oxidation of 1 with 4 Could Proceed via Either Mono- or Bimetallic Pathways^a



^aOxidative addition of X₂ or related oxidants could potentially afford either cis or trans addition products.

followed by monometallic oxidation (c), or by initial bimetallic oxidation of **1** to a binuclear Pd(III) complex (b) followed by Pd–Pd heterolysis (d). Herein, we report data that are consistent with initial oxidation to a bimetallic Pd(III) complex, which undergoes fragmentation to a Pd(IV) and a Pd(II) complex. We discuss the intimate mechanism of fragmentation, which has been derived from computational investigations. Finally, we report an example of fragmentation of a bimetallic Pd(III) complex, which represents the first experimental observation that connects bimetallic Pd(III) and monometallic Pd(IV) chemistry.

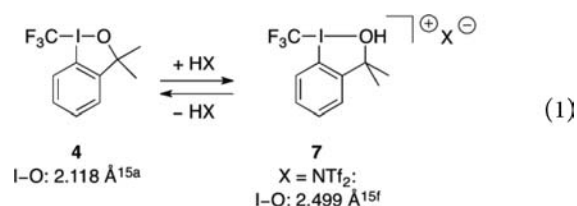
RESULTS

Nuclearity of Oxidation of Pd(II) Complex 1. In solution, Pd(II) complex **1** is binuclear: an upfield shift of the ¹H NMR resonances of the benzo[*h*]quinolinyll protons in **1** as compared to free benzo[*h*]quinoline is observed, which is consistent with close proximity of the aromatic ligands in solution.¹¹ An NOE is observed between H-2 and H-10', confirming that the cyclometalated ligands of **1** are held in proximity in solution (Scheme 2).^{2d} In addition, the observed fidelity of the UV–vis spectral features to Beer's Law confirms that **1** does not aggregate or dissociate in solution.¹²

While complex **1** is binuclear in solution, complex **5**, the product of oxidation, is mononuclear. Potentially, either oxidation by **4**, or fragmentation of a binuclear complex to a mononuclear complex, could be the rate-limiting step in the

formation of **5**. No reaction intermediates were observed by either ¹H or ¹⁹F NMR spectroscopy during the oxidation of **1** to **5**, and thus, we used the method of initial rates to gain insight into the relative timing of the requisite oxidation and fragmentation reactions. The initial rate of oxidation was determined to be first-order dependent on both the concentration of oxidant **4** ([**4**]), as well as the concentration of binuclear Pd(II) complex **1** ([**1**]). If dissociation of **1** to afford two equivalent mononuclear species were to precede rate-determining oxidation, a reaction order of 1/2 with respect to [**1**] would be expected.¹³ We also investigated the order of the reaction in AcOH because the yield of **5** in the oxidation of **1** with **4** is positively correlated with [AcOH].^{8a} The initial rate of oxidation was found to be first-order dependent on the concentration of AcOH ([AcOH]). These experiments afforded an empirically determined rate law: rate = *k*[**1**][**4**][AcOH].

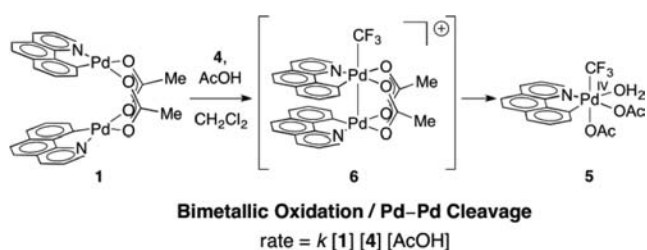
To establish the role of AcOH, potentially functioning as either an acid catalyst or as a source of acetate, a potential nucleophilic catalyst, we examined the competence of AcO[−] as a catalyst for the oxidation of **1**. Acetate is not a competent catalyst for the oxidation of **1** with **4**; no reaction was observed upon treatment of **1** with **4** in the presence of 1.0 equiv of *n*-Bu₄NOAc at 23 °C. The dependence of the reaction rate on [AcOH] but not on [AcO[−]] is consistent with protonation of **4** with AcOH to generate a more potent oxidant (i.e., **7**, X = AcO), which subsequently engages in oxidation of **1**.^{14,15} Consistent with the proposed protonation of **4** by AcOH, the ¹⁹F NMR chemical shift of **4** was observed to monotonically shift downfield with increasing concentration of AcOH, and treatment of **4** with 1.0 equiv of camphor sulfonic acid (CSA), reported to protonate **4**,^{15c} resulted in a downfield shift of the ¹⁹F NMR signal of **4**. Additionally, X-ray crystallographic analysis of **7** (X = NTf₂), obtained by protonation of **4** with HNTf₂, shows protonation of oxygen lengthens the I–O bond (eq 1).^{15f} Similar interactions of hypervalent iodine reagents with Lewis acids, such as Zn(OTf)₂,^{15b} have also been observed.



The experimentally determined rate law for oxidation of **1**, rate = *k*[**1**][**4**][AcOH], is consistent with an oxidized binuclear Pd complex (i.e., **6**) as the immediate product of oxidation of **1** (Scheme 3). In this reaction manifold, initial protonation of **4** to afford **7**, followed by oxidation of **1** by **7**, would lead to the formation of high-valent binuclear cation **6**. Intermediate **6** would then undergo formal Pd–Pd heterolysis to afford mononuclear Pd(IV) complex **5**. In light of the valence asymmetry implicit in **6**, and computational studies elaborating on the subtleties of formal oxidation state assignment for unsymmetrical binuclear Pd(III) species,⁶ formal oxidation states have not been assigned for unsymmetrical species discussed herein.

The rate law for oxidation of **1** with **4** is also consistent with an oxidation pathway in which an acetate ion released on protonation of **4** reacts with **1** to afford a mononuclear

Scheme 3. Mononuclear Pd(IV) **5** is Proposed To Form from Binuclear Pd(II) **1** via Initial Bimetallic Oxidation



palladate species, which subsequently undergoes oxidation by **7** (Scheme 2, path a (acetate-assisted) followed by c). We cannot definitively exclude this possibility; however, evidence suggests against it: acetate is not required for oxidation, and acetic acid can be replaced by CSA in the oxidation of **1** with **4**, resulting in observation of mononuclear Pd(IV) complex **5** in 36% yield based on Pd.

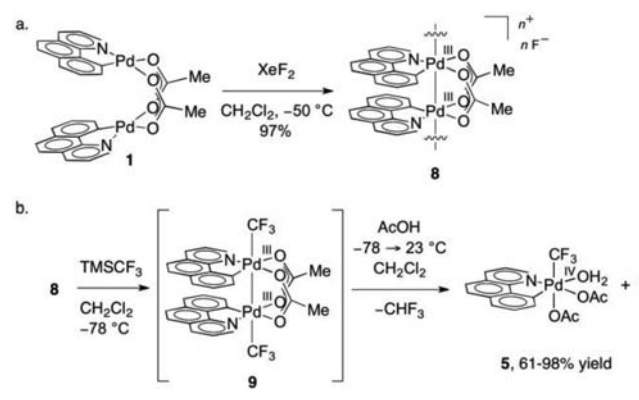
Pd–Pd Cleavage. Formation of mononuclear Pd(IV) complex **5** from **6** requires formal Pd–Pd heterolysis, which would generate both a Pd(IV) complex (**5**) and a Pd(II) complex ($1/2$ equiv of **1**). Heterolytic cleavage of M–M bonds has been observed in binuclear Pt(III) complexes,¹⁶ but has not yet been established in dipalladium(III) chemistry. Proposed intermediate **6** was not observed during oxidation of **1** with **4**, presumably because Pd–Pd heterolysis is significantly faster than oxidation of **1** with **4**.

While we have not observed a binuclear Pd(III) complex during the oxidation of **1** with **4**, we have experimentally observed Pd(III)–Pd(III) bond cleavage under modified conditions. Previously, we have shown that treatment of Pd(III) complex **8**, generated by oxidation of **1** with XeF₂,¹⁷ with either TMSCl or TMSOAc affords characterized binuclear Pd(III) complexes **2** and **3**, respectively. In an effort to generate a binuclear Pd(III) trifluoromethyl complex (i.e., **9**), Pd(III) wire **8** was treated with 3.0 equiv of TMSCF₃. Consumption of **8** and formation of an intermediate was detected by ¹H NMR spectroscopy. While the instability of this species precluded full characterization, the available evidence is consistent with it being Pd(III) trifluoromethyl complex **9**. The assignment of the structure of **9** is based on analogy to the reaction of **8** with other TMSX reagents, which affords binuclear Pd(III) complexes (Scheme 2, reaction a). In addition, the ¹H NMR spectrum of **9** contains a signal at 2.74 ppm, consistent with the bridging acetate resonance of other binuclear Pd(III) complexes. Both of these pieces of data are consistent with all other benzo[*h*]quinolinyl acetate-bridged Pd(III) complexes that have been prepared.^{2a,b}

Treatment of the reaction mixture containing complex **9** with 10.0 equiv of AcOH and warming from $-78 \rightarrow 23$ °C resulted in the formation of mononuclear Pd(IV) complex **5** in 61–98% yield,¹⁸ as well as complex **1** (74–89%), HCF₃ (21–30% yield, based on ¹⁹F NMR spectroscopy), and TMSF (40–52%) (Scheme 4b).¹⁹ The formation of **5** by sequential treatment of Pd(III) complex **8** with TMSCF₃ and AcOH confirms the viability of formal Pd–Pd heterolysis to generate mononuclear Pd(IV) complexes.

Computational Investigations. Direct interrogation of the mechanism of Pd–Pd heterolysis by experiment is challenging because fragmentation of **6** occurs after the rate-determining step of oxidation of **1** with **4**. To probe the nature

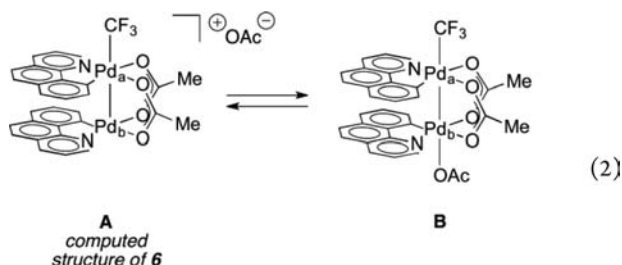
Scheme 4. (a) Oxidation of Binuclear Pd(II) Complex **1** with XeF₂ Affords Pd(III) Wire **8** and (b) Treatment of Pd(III) Wire **8** with TMSCF₃ and AcOH Afforded Mononuclear Pd(IV) Complex **5** and Binuclear Pd(II) Complex **1**, the Products Expected of Pd–Pd Heterolysis



of the fragmentation process, computational studies of this transformation have been undertaken.

Computation was carried out using identical procedures as were used in a recent study of C–Cl reductive elimination from the binuclear benzo[*h*]quinolinyl complex **3** with dichloromethane as a solvent.⁶ Gaussian 09²⁰ was used at the M06 level of density functional theory (DFT); selected species were also examined using the BP86, TPSS, and wB97XD functionals.²¹ The effective core potential of Hay and Wadt with a triple- ξ valence basis set (LAN2TZ) was chosen to describe Pd,²² the 6-31G(d) basis set was used for other atoms,²³ and a polarization function of $\xi_f = 1.472$ was also added to Pd to form basis set BS1.²⁴ Frequency calculations were carried out at the BS1 level. To further refine energies obtained from the M06/BS1 calculations, we carried out single point energy calculations for all the structures with a larger basis set (BS2) utilizing the quadruple- ξ valence polarized def2-QZVP basis set²⁵ on Pd along with the corresponding ECP and the 6-311+G(2d,p) basis set on other atoms. The CPCM solvation model²⁶ was used to calculate solvation energies using BS2 and gas-phase-optimized geometries. To estimate the corresponding solvated Gibbs free energies (ΔG), entropy corrections were calculated at the gas phase M06/BS1 level and added to the solvent potential energies.²⁷ To provide more precise Pd–O bond dissociation energies, basis set superposition errors (BSSE) were evaluated. The nature of transition structures was confirmed by intrinsic reaction coordinate (IRC) searches, vibrational frequency calculations, and potential energy surface scans. In the following discussion, computed structures will be referred to with compound letters, not numbers; for example, the computed structure of binuclear cation **6** will be referred to as **A**.

Structure of 6. The rate law of oxidation implicates binuclear cation **6** as the immediate product of oxidation of **1** with **4**. Because oxidation is carried out in the presence of AcOH, we evaluated potential binding of AcO[−] to the binuclear core of **A** to generate neutral, binuclear Pd(III) trifluoromethyl acetate complex **B**. We have computed the association of **A** with AcO[−] to be approximately thermoneutral using the CPCM solvation model²⁶ for CH₂Cl₂ (eq 2). Because of the accessibility of both cationic and neutral binuclear Pd(III) structures, both have been evaluated with regard to fragmentation and reductive elimination pathways (*vide infra*).



Fragmentation of the Pd–Pd Core. We identified a low-energy pathway for the fragmentation of neutral binuclear Pd(III) complex **B** by scanning the potential energy surface as a function of increasing Pd–Pd separation (Scheme 5). Starting with a Pd–Pd separation of 2.692 Å, computed for the gas-phase structure of **B**, transition structure **C**, which connects structure **B** with isomer **D**, was located. Isomer **D** has a Pd–Pd distance 0.15 Å longer than **B**, and only one bridging acetate coordinated trans to carbon at the Pd_a–R center and trans to nitrogen at Pd_b.²⁸ Continued elongation of the Pd–Pd distance of **D** led to identification of structures **F** and **G**. Structure **G** evolves to **H** and **I**, the products of Pd–Pd cleavage. The conversion of **D** to **F** proceeds via structure **E**, which was identified as the highest energy point between **D** and **F**, but could not be optimized as a transition structure.²⁹ Structure **E** is included to illustrate the path of isomerization of **D** to **F**. Structure **G**, in which there is a weak Pd_b⋯O interaction (2.912 Å), can be confidently assessed as the species leading to structurally characterized Pd(IV) structure **H** (**5**), with the accompanying Pd(II) species **I** (**1**), which were computed to have a combined energy of ΔG (ΔH) = –3.9 (12.8) kcal mol^{–1}. Subsequent reaction of the resulting Pd(II) complex **I** with **4** can afford additional mononuclear Pd(IV) complex **5**.

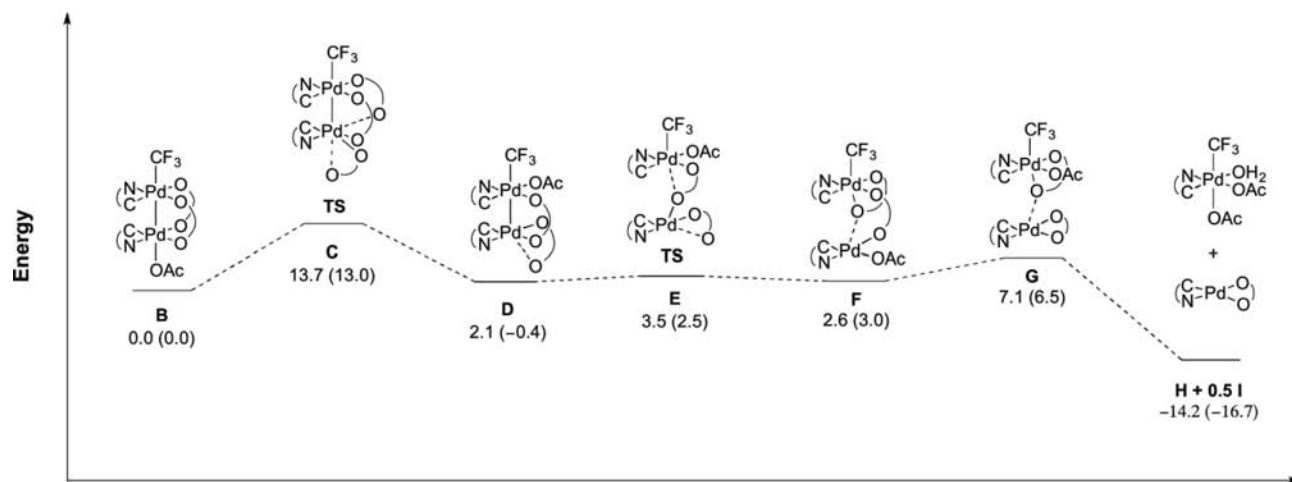
Similar computational analysis of potential fragmentation of the binuclear cation **A** led to steadily increasing energy to values >24 kcal mol^{–1} (BS1, gas phase **E**) at a Pd_a⋯Pd_b distance of 4.7 Å with retention of strong acetate bridging between Pd_a and Pd_b. An inflection at ~3.8 Å allowed optimization of a high energy species (ΔG 22.4 kcal mol^{–1}) exhibiting a Pd_a⋯Pd_b distance of 3.861 Å. Both acetates retain their bridging role with

normal Pd–O distances, and in addition the oxygen atom trans to carbon at Pd_b now also bridges to Pd_a resulting in a pseudo-octahedral Pd(IV) center at Pd_a and square-planar Pd(II) center at Pd_b (Pd_a–O 2.365 Å, Pd_b–O 2.308 Å). In view of the high energy of this optimized species, and in the absence of fragmentation at longer Pd_a⋯Pd_b separations at even higher energy, it is most likely that fragmentation occurs from **B**.

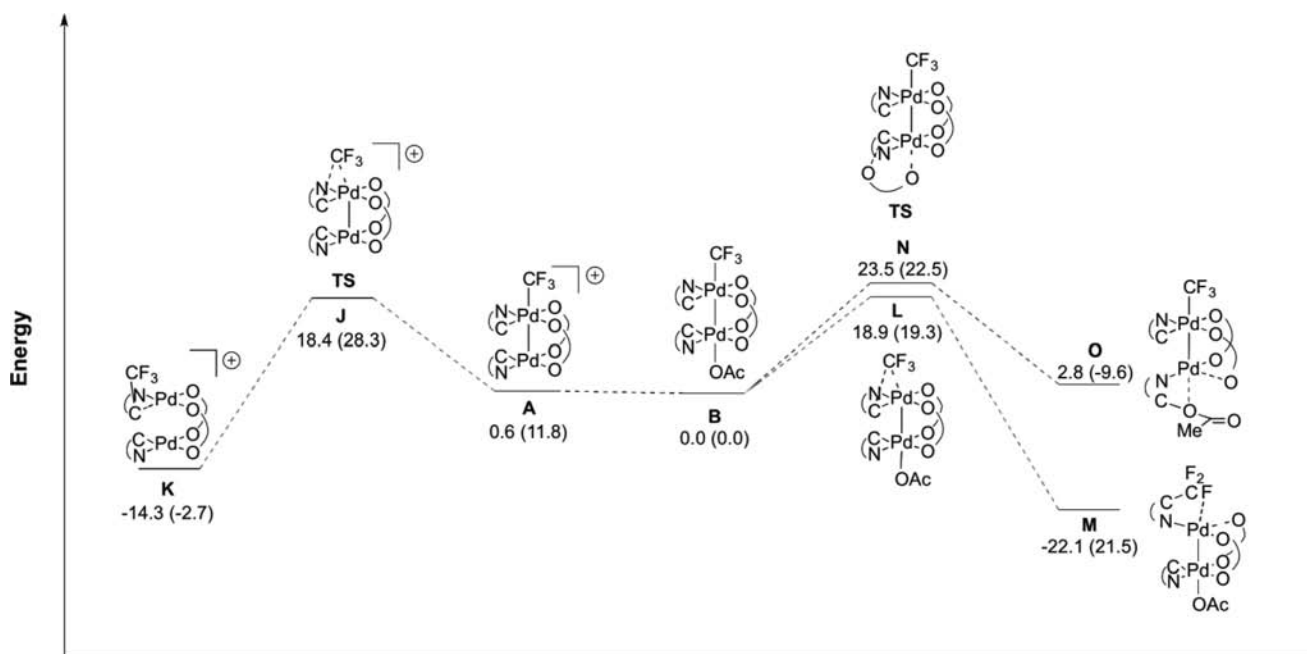
Potential Reductive Elimination from the Binuclear Core. After identification of the fragmentation pathway illustrated in Scheme 5, we examined potential reductive elimination reactions from either **A** or **B** to ascertain whether there may be other low energy reaction pathways for the decomposition of binuclear Pd(III) trifluoromethyl complexes. Scheme 6 illustrates the pathways for C–CF₃ reductive elimination from binuclear complex **A** that were identified by IRC searches. We identified transition structure **J** for C–CF₃ reductive elimination from cation **A** (Scheme 7). Transition structure **J** connects binuclear cation **A** with complex **K**, best described as containing a Pd(II) center with a bound arenonium, in which the C–CF₃ bond is formed.³⁰ The Pd–Pd distance increases from **A** to **K**, which is consistent with cleavage of the Pd–Pd bond during reductive elimination.³¹ We also evaluated potential reductive elimination from neutral binuclear Pd(III) structure **B**. Transition structures **N** and **L** were identified for the reductive elimination of C–OAc and C–CF₃ bonds, respectively.³² Transition structure **N** is similar to transition structures for C–OAc reductive elimination identified in a recent computational study of C–OAc reductive elimination from **3**.³³

The observation that transition structure **N**, for C–OAc reductive elimination, is higher in energy than transition structure **L**, for C–CF₃ reductive elimination, may be at least partly influenced by valence asymmetry of the binuclear core. Computed C–CF₃ reductive elimination originates from a Pd center that resembles Pd(IV) while computed C–OAc reductive elimination originates from a Pd center that has partial Pd(II) character. Both pathways were found to proceed through a transition structure significantly higher in energy than the transition structures associated with Pd–Pd fragmentation. Additional calculations have been performed with the BP86,

Scheme 5. Reaction Coordinate Analysis for the Fragmentation of **B** to Mononuclear Pd(IV) Complex **5** (**H**) and Pd(II) Complex **1** (**I**)^a

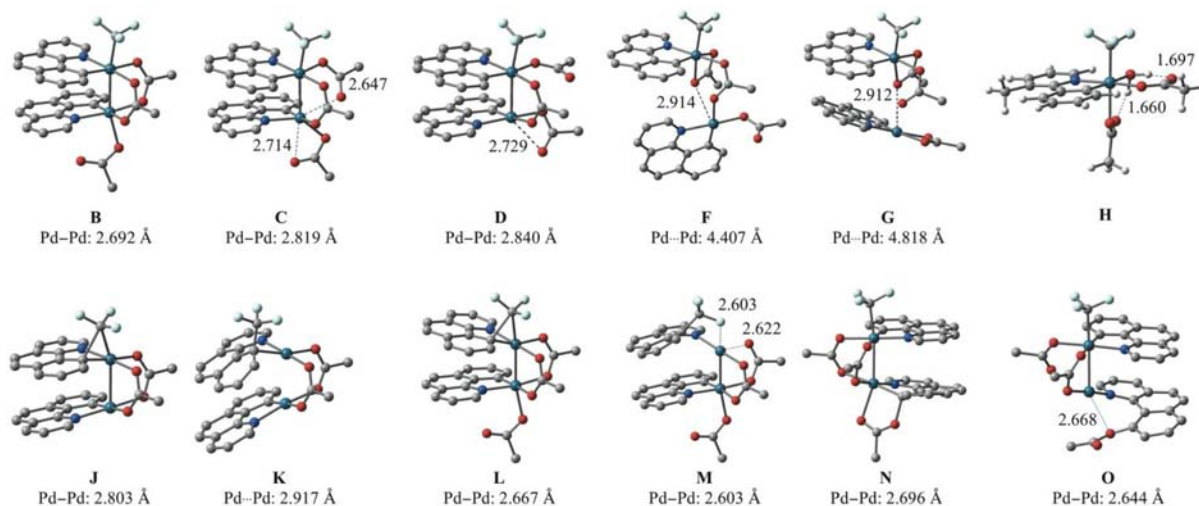


^aAll calculations are carried out with the appropriate number of ancillary molecules to balance the chemical equations. The calculated relative energies (and enthalpies) are given in kcal mol^{–1}.

Scheme 6. Reaction Coordinate Analysis for Potential C–CF₃ and C–OAc Reductive Elimination Reactions from Binuclear Pd(III) Structures A and B^a

^aThe calculated relative energies (and enthalpies) are given in kcal mol⁻¹.

Scheme 7. Computed Structures Involved in Potential Fragmentation (Scheme 5) and Reductive Elimination (Scheme 6) Processes



TPSS, and wB97XD density functionals, and similar trends in the reaction barriers have been observed (see Supporting Information). While the absolute transition state energies vary between the functionals, the M06, BP86, and wB97XD functionals all agree that fragmentation via transition state C is preferred over reductive elimination via transition state J, L, or N, respectively.

DISCUSSION

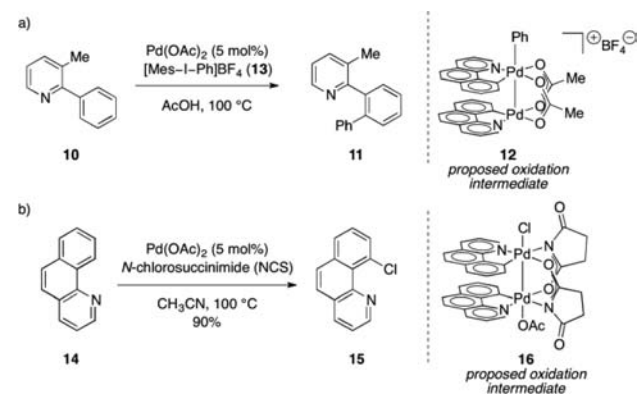
The nuclearity of high-valent Pd intermediates in C–H oxidation catalysis has recently been the topic of discussion.^{4,5} Both binuclear Pd(III) and mononuclear Pd(IV) complexes have been proposed as high-valent intermediates in catalysis. Historically, mechanisms proceeding through mononuclear

Pd(IV) intermediates and binuclear Pd(III) intermediates have been presented as mechanistic alternatives, and potential connections between these limiting catalysis cycles have not been discussed. Formation of a mononuclear Pd(IV) complex from Pd(III) complex 8, reported herein, demonstrates that both Pd(III) and Pd(IV) can be accessed under similar conditions and allows potential mechanistic nuances to be elucidated.³⁴

While oxidation of complex 1 with hypervalent iodine reagents PhICl₂ and PhI(OAc)₂ affords isolable binuclear Pd(III) complexes 2 and 3, respectively,² oxidation of 1 with hypervalent iodine reagent 4 affords mononuclear Pd(IV) complex 5. Despite the different nuclearities of products resulting from oxidation of 1 with hypervalent iodine reagents, monitoring the reaction kinetics of oxidation indicates that each

of these three reactions proceeds by initial oxidation to a binuclear Pd complex. The rate law of Pd(OAc)₂-catalyzed C–H arylation, rate = $k[\text{Pd}]^2[\mathbf{13}][\mathbf{10}]^{-3}$, in combination with the spectroscopically observed mononuclear Pd(II) catalyst resting state, implicates binuclear intermediates in oxidation during the reaction in Scheme 8a.^{2c} The rate law of Pd(OAc)₂-catalyzed

Scheme 8. (a) Rate Law of Oxidation, Combined with the Spectroscopically Observed Catalyst Resting State, Implicates Binuclear Oxidation Intermediate **12 During Pd-Catalyzed C–H Arylation, and (b) Acetate-Assisted Oxidation During Pd-Catalyzed C–H Chlorination Is Proposed To Generate **16** as the Immediate Product of Oxidation During Catalysis**



C–H chlorination of 2-phenylpyridine derivatives was determined to be rate = $k[\text{Pd}_2][\text{NCS}][\text{AcO}^-]$, which is consistent with rate-determining, acetate-assisted oxidation of a binuclear Pd complex (Scheme 8b).^{2d} Similarly, oxidation of binuclear Pd(II) complex **1** with **4** to afford mononuclear Pd(IV) complex **5** likely proceeds through initial oxidation of a binuclear complex. The observed dichotomy between oxidation reactions of complex **1** that afford binuclear Pd(III) complexes versus mononuclear Pd(IV) complexes is not due to differences in oxidation, but due to reactivity differences of the initially formed binuclear Pd(III) complexes. While binuclear Pd(III) complexes **2** and **3** have been isolated, the accumulated evidence is consistent with binuclear intermediate **6** undergoing facile Pd–Pd cleavage to afford mononuclear Pd(IV) complex **5**.

Computational examination of potential pathways available for the decomposition of **B** revealed that a facile reaction manifold for Pd–Pd heterolysis is available. The sequence **B** (Pd–Pd 2.692 Å) to **G** (Scheme 5) indicates that fragmentation occurs via a succession of acetate group rearrangements: one bridge becomes unidentate at Pd_a, and the axial acetate at Pd_b moves to the square plane and retains a weak axial interaction to give **D** (Pd–Pd 2.840 Å); the unidentate acetate at Pd_a becomes bidentate and develops a weak Pd_b...O interaction as the Pd–Pd bond breaks to form **F** (Pd...Pd 4.407 Å). Finally, the remaining bridging acetate becomes unidentate at Pd_a, and the unidentate acetate at Pd_b becomes bidentate in **G** (Pd...Pd 4.818 Å). During this process Pd_a and Pd_b gradually adopt coordination geometries consistent with disproportionation, completed at **F**, resulting in pseudo-octahedral Pd(IV) and pseudosquare planar Pd(II) centers in **F** and **G**. Fragmentation of **G** is followed by dimerization of the resulting Pd(II) species to afford **I** and coordination of water to the Pd(IV) center to afford **H**.

In 2010, Canty and Yates proposed that binuclear Pd(III) complexes bearing apical ligands of differing σ -donating ability, such as **B**, should be formulated as mixed-valence Pd(IV)/Pd(II) \leftrightarrow Pd(III)/Pd(III) dimers rather than valence symmetric Pd(III) dimers.^{6,35} Pd–Pd heterolysis is the limiting case of valence localization in a binuclear complex. Formation of **5** from **8** confirms the viability of Pd–Pd bond heterolysis as a pathway to access mononuclear Pd(IV) complexes by formal heterolysis of Pd(III)–Pd(III) bonds and is consistent with recently reported computational investigations of the valence asymmetry of binuclear Pd(III) complexes.^{6,35} The specific electronic and structural parameters that favor fragmentation over C–X coupling from a binuclear core remain to be established.

CONCLUSION

A growing body of research points to the importance of binuclear Pd(III) intermediates in C–H oxidation chemistry. Two studies are available that provide experimentally derived insight into the nature of the oxidation step during catalysis. Both studies indicate the intermediacy of binuclear intermediates in catalysis, and both have a ligand frequently employed in Pd-catalysis (acetate) present in a key metal-bridging role.^{2c,d} In light of the importance of C–CF₃ bond-forming reactions, and the recent observation of mononuclear Pd(IV) complexes during model reactions (Scheme 1), we have obtained data relevant to the mechanism of formation of **5** to gain insight into the relative roles of mono- and binuclear intermediates. The results of this investigation are consistent with a two-step, oxidation–disproportionation sequence for the formation of **5** in which the initial product of oxidation is binuclear Pd(III) complex **6**. We hypothesize that bimetallic oxidation of **1** (b, Scheme 3) may be favored over potential oxidation of mononuclear Pd(II) complexes to Pd(IV) complex **5** (d) because Pd–Pd bond formation occurs during oxidation and lowers the activation barrier to oxidation.⁵

The observed fragmentation of **6** illustrates the complexities in mechanisms available for arene functionalization via higher oxidation state palladium intermediates. While symmetric complexes, such as **2**, undergo facile C–X reductive elimination chemistry without prior cleavage of the binuclear core, binuclear Pd(III) complex **6** fragments to Pd(IV) and Pd(II) complexes. Canty and Yates have provided a theoretical model with which to describe this fragmentation, which is based on valence asymmetry of binuclear complexes bearing different apical ligands.^{6,35} It remains to be defined where on the continuum of ligand donating ability Pd–Pd cleavage becomes competitive with C–X reductive elimination from binuclear intermediates.

ASSOCIATED CONTENT

Supporting Information

Detailed experimental procedures, spectroscopic data for all new compounds, complete ref 20, energy parameters, and Cartesian coordinates of all optimized structures. Crystallographic data for **1** and **5** (CIF). This material is available free of charge via the Internet at <http://pubs.acs.org>.

AUTHOR INFORMATION

Corresponding Author

Allan.Canty@utas.edu.au; Brian.Yates@utas.edu.au; ritter@chemistry.harvard.edu

Notes

The authors declare no competing financial interest.

ACKNOWLEDGMENTS

We thank D. Ford (Harvard) for helpful discussions, A. Togni and E. Maennel (ETH Zurich) for helpful discussions and providing unpublished data concerning the X-ray crystal structure of compound 7, S.-L. Zheng and T. M. Powers (Harvard) for X-ray crystallographic analysis, the Australian National Computational Infrastructure and the University of Tasmania for computing resources, the AFOSR (FA9550-10-1-0170), the NSF (CHE-0952753 and CHE-1111563), and the Australian Research Council for financial support.

REFERENCES

- (1) (a) Canty, A. J.; Watson, A. A.; Skelton, B. W.; White, A. H. *J. Organomet. Chem.* **1989**, *367*, C25–C28. (b) Alsters, P. L.; Engel, P. F.; Hogerheide, M. P.; Copijn, M.; Spek, A. L.; van Koten, G. *Organometallics* **1993**, *12*, 1831–1844. (c) van Asselt, R.; Rijnberg, E.; Elsevier, C. J. *Organometallics* **1994**, *13*, 706–720. (d) Vicente, J.; Chicote, M.-T.; Lagunas, M.-C.; Jones, P. G.; Bembenek, E. *Organometallics* **1994**, *13*, 1243–1250. (e) van Belzen, R.; Hoffmann, H.; Elsevier, C. J. *Angew. Chem., Int. Ed.* **1997**, *36*, 1743–1745. (f) Canty, A. J.; Hoare, J. L.; Davies, N. W.; Traill, P. R. *Organometallics* **1998**, *17*, 2046–2051. (g) Yamamoto, Y.; Ohno, T.; Itoh, K. *Angew. Chem., Int. Ed.* **2002**, *41*, 3662–3665. (h) Dick, A. R.; Kampf, J. W.; Sanford, M. S. *J. Am. Chem. Soc.* **2005**, *127*, 12790–12791. (i) Whitfield, S. R.; Sanford, M. S. *J. Am. Chem. Soc.* **2007**, *129*, 15142–15143. (j) Fu, Y.; Li, Z.; Liang, S.; Guo, Q.-X.; Liu, L. *Organometallics* **2008**, *27*, 3736–3742. (k) Furuya, T.; Ritter, T. *J. Am. Chem. Soc.* **2008**, *130*, 10060–10061. (l) Racowski, J. M.; Dick, A. R.; Sanford, M. S. *J. Am. Chem. Soc.* **2009**, *131*, 10974–10983. (m) Arnold, P. L.; Sanford, M. S.; Pearson, S. M. *J. Am. Chem. Soc.* **2009**, *131*, 13912–13913. (n) Furuya, T.; Benitez, D.; Tkatchouk, E.; Strom, A. E.; Tang, P.; Goddard, W. A., III; Ritter, T. *J. Am. Chem. Soc.* **2010**, *132*, 3793–3807. (o) Oloo, W.; Zavali, P. Y.; Zhang, J.; Khaskin, E.; Vedernikov, A. N. *J. Am. Chem. Soc.* **2010**, *132*, 14400–14402.
- (2) (a) Powers, D. C.; Ritter, T. *Nat. Chem.* **2009**, *1*, 302–309. (b) Deprez, N. R.; Sanford, M. S. *J. Am. Chem. Soc.* **2009**, *131*, 11234–11241. (c) Powers, D. C.; Geibel, M. A. L.; Klein, J. E. M. N.; Ritter, T. *J. Am. Chem. Soc.* **2009**, *131*, 17050–17051. (d) Powers, D. C.; Xiao, D. Y.; Geibel, M. A. L.; Ritter, T. *J. Am. Chem. Soc.* **2010**, *132*, 14530–14536. (e) Powers, D. C.; Benitez, D.; Tkatchouk, E.; Goddard, W. A.; Ritter, T. *J. Am. Chem. Soc.* **2010**, *132*, 14092–14103. (f) Powers, D. C.; Ritter, T. *Top. Organomet. Chem.* **2011**, *35*, 129–156.
- (3) (a) Henry, P. M. *J. Org. Chem.* **1971**, *36*, 1886–1890. (b) Stock, L. M.; Tse, K.; Vorvick, L. J.; Walstrum, S. A. *J. Org. Chem.* **1981**, *46*, 1757–1759. (c) Yoneyama, T.; Crabtree, R. H. *J. Mol. Catal. A: Chem.* **1996**, *108*, 35–40. (d) Dick, A. R.; Hull, K. L.; Sanford, M. S. *J. Am. Chem. Soc.* **2004**, *126*, 2300–2301. (e) Kalyani, D.; Dick, A. R.; Anani, W. Q.; Sanford, M. S. *Tetrahedron* **2006**, *62*, 11483–11498.
- (4) Reviews: (a) Alberico, D.; Scott, M. E.; Lautens, M. *Chem. Rev.* **2007**, *107*, 174–238. (b) Daugulis, O.; Do, H.-Q.; Shabashov, D. *Acc. Chem. Res.* **2009**, *42*, 1074–1086. (c) Chen, X.; Engle, K. M.; Wang, D.-H.; Yu, J.-Q. *Angew. Chem., Int. Ed.* **2009**, *48*, 5094–5115. (d) Muñiz, K. *Angew. Chem., Int. Ed.* **2009**, *48*, 9412–9423. (e) Xu, L.-M.; Li, B.-J.; Yang, Z.; Shi, Z.-J. *Chem. Soc. Rev.* **2010**, *39*, 712–733. (f) Sehnal, P.; Taylor, R. J. K.; Fairlamb, I. J. S. *Chem. Rev.* **2010**, *110*, 824–889. (g) Lyons, T. W.; Sanford, M. S. *Chem. Rev.* **2010**, *110*, 1147–1169.
- (5) Powers, D. C.; Ritter, T. *Acc. Chem. Res.* **2012**, *45*, 840–850.
- (6) Ariafard, A.; Hyland, C. J. T.; Canty, A. J.; Sharma, M.; Yates, B. F. *Inorg. Chem.* **2011**, *50*, 6449–6457.
- (7) Eisenberger, P.; Gisichig, S.; Togni, A. *Chem.—Eur. J.* **2006**, *12*, 2579–2586.
- (8) (a) Ye, Y.; Ball, N. D.; Kampf, J. W.; Sanford, M. S. *J. Am. Chem. Soc.* **2010**, *132*, 14682–14687. For the original report of directed Pd(OAc)₂-catalyzed trifluoromethylation, see (b) Wang, X.; Truesdale, L.; Yu, J.-Q. *J. Am. Chem. Soc.* **2010**, *132*, 3648–3649.
- (9) Trifluoromethyl Pd(IV) complexes supported by bipyridyl ligands have been reported: (a) Ball, N. D.; Kampf, J. W.; Sanford, M. S. *J. Am. Chem. Soc.* **2010**, *132*, 2878–2879. (b) Ball, N. D.; Gary, J. B.; Ye, Y.; Sanford, M. S. *J. Am. Chem. Soc.* **2011**, *133*, 7577–7584. (c) Maleckis, A.; Sanford, M. S. *Organometallics* **2011**, *30*, 6617–6627. (d) Racowski, J. M.; Ball, N. D.; Sanford, M. S. *J. Am. Chem. Soc.* **2011**, *133*, 18022–18025.
- (10) Ryabov, A. D. *Inorg. Chem.* **1987**, *26*, 1252–1260.
- (11) (a) Gutierrez, M. A.; Newkome, G. R.; Selbin, J. J. *Organomet. Chem.* **1980**, *202*, 341–350. (b) Navarro-Ranninger, C.; Zamora, F.; Martínez-Cruz, L. A.; Isea, R.; Masaguer, J. R. *J. Organomet. Chem.* **1996**, *518*, 29–36.
- (12) (a) Jennette, K. W.; Gill, J. T.; Sadowick, J. A.; Lippard, S. J. *J. Am. Chem. Soc.* **1976**, *98*, 6159–6168. (b) Bailey, J. A.; Hill, M. G.; Marsh, R. E.; Miskowski, V. M.; Schaefer, W. P.; Gray, H. B. *Inorg. Chem.* **1995**, *34*, 4591–4599. (c) Yam, V. W.-W.; Yu, K.-L.; Cheung, K.-K. *J. Chem. Soc., Dalton Trans.* **1999**, 2913–2915. (d) Wong, K. M.-C.; Zhu, N. Y.; Yam, V. W.-W. *Chem. Commun.* **2006**, 3441–3443. (e) Lo, L. T.-L.; Ng, C.-O.; Feng, H.; Ko, C.-C. *Organometallics* **2009**, *28*, 3597–3600.
- (13) (a) Chan, Y. N. C.; Osborn, J. A. *J. Am. Chem. Soc.* **1990**, *112*, 9400–9401. (b) Louie, J.; Hartwig, J. F. *J. Am. Chem. Soc.* **1995**, *117*, 11598–11599. (c) Driver, M. S.; Hartwig, J. F. *J. Am. Chem. Soc.* **1997**, *119*, 8232–8245. (d) Vazquez-Serrano, L. D.; Owens, B. T.; Buriak, J. M. *Inorg. Chim. Acta* **2006**, *359*, 2786–2797. (e) Fulmer, G. R.; Muller, R. P.; Kemp, R. A.; Goldberg, K. I. *J. Am. Chem. Soc.* **2009**, *131*, 1346–1347.
- (14) The proposed reaction of **4** with AcOH prior to oxidation of **1** is expected to result in saturation kinetics with respect to AcOH. At the concentrations of AcOH that were employed in reaction kinetics experiments, saturation was not observed.
- (15) (a) Kietlsch, I.; Eisenberger, P.; Togni, A. *Angew. Chem., Int. Ed.* **2007**, *46*, 754–757. (b) Koller, R.; Stanek, K.; Stolz, D.; Aardoom, R.; Niedermann, K.; Togni, A. *Angew. Chem., Int. Ed.* **2009**, *48*, 4332–4336. (c) Koller, R.; Huchet, Q.; Battaglia, P.; Welch, J. M.; Togni, A. *Chem. Commun.* **2009**, 5993–5995. (d) Allen, A. E.; MacMillan, D. W. C. *J. Am. Chem. Soc.* **2010**, *132*, 4986–4987. (e) Niedermann, K.; Früh, N.; Senn, R.; Czarniecki, B.; Verel, R.; Togni, A. *Angew. Chem., Int. Ed.* **2012**, *51*, 6511–6515. (f) Togni, A. Personal communication and CCDC875434.
- (16) (a) Bandoli, G.; Caputo, P. A.; Intini, F. P.; Sivo, M. F.; Natile, G. *J. Am. Chem. Soc.* **1997**, *119*, 10370–10376. (b) Bonnington, K. J.; Jennings, M. C.; Puddephatt, R. J. *Organometallics* **2008**, *27*, 6521–6530. (c) Canty, A. J.; Gardiner, M. G.; Jones, R. C.; Rodemann, T.; Sharma, M. *J. Am. Chem. Soc.* **2009**, *131*, 7236–7237. (d) Unobserved Pd(III)–Pd(III) intermediates have recently been proposed in the electrochemical oxidation of Pd(II) to Pd(IV): Luo, J.; Khusnutdinova, J. R.; Rath, N. P.; Mirica, L. M. *Chem. Commun.* **2012**, *48*, 1532–1534.
- (17) Campbell, M. G.; Powers, D. C.; Raynaud, J.; Graham, M. J.; Xie, P.; Lee, E.; Ritter, T. *Nat. Chem.* **2011**, *3*, 949–953.
- (18) A range of yields is reported for the reaction of **8** with TMSCF₃ because the reaction yields have been observed to vary significantly based on variables that we have not identified.
- (19) The aquo ligand of **5** is likely introduced with the AcOH, which was not dried prior to use.
- (20) Frisch, M. J.; et al. *Gaussian 09, revision A.02*; Gaussian, Inc.: Wallingford, CT, 2009.
- (21) (a) Zhao, Y.; Schultz, N. E.; Truhlar, D. G. *J. Chem. Theory Comput.* **2006**, *2*, 364–382. (b) Zhao, Y.; Truhlar, D. G. *J. Chem. Phys.* **2006**, *125*, 194101. (c) Zhao, Y.; Truhlar, D. G. *J. Phys. Chem. A* **2006**, *110*, 13126–13130.
- (22) (a) Hay, P. J.; Wadt, W. R. *J. Chem. Phys.* **1985**, *82*, 270–273. (b) Wadt, W. R.; Hay, P. J. *J. Chem. Phys.* **1985**, *82*, 284–298. (c) Roy, L. E.; Hay, P. J.; Martin, R. L. *J. Chem. Theory Comput.* **2008**, *4*, 1029–1031.

(23) Hariharan, P. C.; Pople, J. A. *Theor. Chim. Acta* **1973**, *28*, 213–222.

(24) Ehlers, A. W.; Böhme, M.; Dapprich, S.; Gobbi, A.; Höllwarth, A.; Jonas, V.; Köhler, K. F.; Stegmann, R.; Veldkamp, A.; Frenking, G. *Chem. Phys. Lett.* **1993**, *208*, 111–114.

(25) Weigend, F.; Furche, F.; Ahlrichs, R. *J. Chem. Phys.* **2003**, *119*, 12753–12762.

(26) Barone, V.; Cossi, M. *J. Phys. Chem. A* **1998**, *102*, 1995–2001.

(27) Wei, C. S.; Jiménez-Hoyos, C. A.; Videa, M. F.; Hartwig, J. F.; Hall, M. B. *J. Am. Chem. Soc.* **2010**, *132*, 3078–3091.

(28) Computation for C–C reductive elimination from isomer **D** gave a transition structure with an energy very similar to **L**, and for which an IRC search confirmed the structure and provided a structure for the C–C coupled product that is similar to **M**.

(29) This point has a low single imaginary frequency (-23 cm^{-1}), which suggests that the potential energy surface should be flat. Atom movements for this frequency are as expected for the transition structure, but attempted transition structure optimization led to the isomer **D**, and optimization at later points in the scan led to **F**.

(30) (a) Formulation of **K** as an arenonium species is supported by presence of a short Pd–C_{ipso} interaction (2.226 Å), C_{ipso}–C distances (1.417, 1.452 Å) that are longer than other C–C distances within the C₆ ring (1.389, 1.389, 1.408, 1.410 Å), and C_{ipso} being well removed from the plane of the ring forming a C_{para}–C_{ipso}–CF₃ angle of 133.5°. Lengthening the Pd–C_{ipso} distance to beyond that for bonding, followed by optimization (**K**), results in a higher energy for the resultant structure (**K'**) [ΔG (ΔH) = -8.6 (-2.2) kcal mol⁻¹] and a strong Pd...F interaction (2.205 Å). (b) Grove, D. M.; van Koten, G.; Ubbels, H. J. C. *Organometallics* **1982**, *1*, 1366–1370.

(31) Pd_a–Pd_b: 2.747 (**A**), 2.803 (**J**), 2.917 (**K**)

(32) The changes in Pd–Pd distance for C–C reductive elimination from cation **A** (**B** → **J**) and neutral species **B** (**B** → **L** → **M**) are very similar to those discussed in detail for the phenyl analogue of **A** and the phenyl(chloro)- analogue of **B**,⁶ and are not discussed here in view of the absence of direct C–C reductive elimination from **A** and **B** as a component of the overall reaction.

(33) Gary, J. B.; Sanford, M. S. *Organometallics* **2011**, *30*, 6143–6149.

(34) The formation of mononuclear Pd(IV) complex **5** by oxidation of **1** with **4** does not provide information regarding the structure of the intermediate from which C–CF₃ bond formation proceeds. Preliminary reaction kinetics measurements, reported in ref 8a (*e.g.*, observation of an induction period under many conditions) suggest that the mechanism of C–CF₃ bond formation may be more complicated than direct reductive elimination from **5**.

(35) Ariafard, A.; Hyland, C. J. T.; Canty, A. J.; Sharma, M.; Brookes, N. J.; Yates, B. F. *Inorg. Chem.* **2010**, *49*, 11249–11253.